Gallate semiquinone radical tri-anion

Experimental and theoretical studies of the ^{13}C hyperfine coupling constants

Pedersen, Jens Arne; Spanget-Larsen, Jens

Published in:
Journal of Molecular Structure

DOI:
10.1016/j.molstruc.2021.130663

Publication date:
2021

Document Version
Publisher's PDF, also known as Version of record

Citation for published version (APA):
Pedersen, J. A., & Spanget-Larsen, J. (2021). Gallate semiquinone radical tri-anion: Experimental and theoretical studies of the ^{13}C hyperfine coupling constants. *Journal of Molecular Structure*, *1241*, Article 130663. https://doi.org/10.1016/j.molstruc.2021.130663

Journal of Molecular Structure 1241 (2021) 130663

Contents lists available at ScienceDirect

Journal of Molecular Structure

journal homepage: www.elsevier.com/locate/molstr

Gallate semiquinone radical tri-anion. Experimental and theoretical studies of the ^{13}C hyperfine coupling constants

Jens Arne Pedersen[a,§], Jens Spanget-Larsen[b,*]

[a] Department of Chemistry, Aarhus University, DK-8000 Aarhus C, Denmark
[b] Department of Science and Environment, Roskilde University, DK-4000 Roskilde, Denmark

ARTICLE INFO

Article history:
Received 5 April 2021
Revised 3 May 2021
Accepted 7 May 2021
Available online 18 May 2021

Keywords:
Gallic acid (GA)
Semiquinone anion
Electron paramagnetic resonance (EPR)
^{13}C hyperfine splittings (HFS)
Karplus-Fraenkel theory
Density functional theory (DFT)

ABSTRACT

Gallic acid (3,4,5-trihydroxybenzoic acid, GA) is one of the most abundant phenolic acids found in the plant kingdom. In this work, the electron paramagnetic resonance (EPR) spectrum of the gallate semiquinone radical tri-anion (GAS) derived from GA by air oxidation was measured and analyzed by advanced simulation procedures. The observed main spectrum was surrounded by five satellite spectra from which a thorough analysis led to determination of hyperfine splittings (HFS) from five chemically different ^{13}C nuclei in natural abundance. The spectra were further characterized by detailed linewidth analyses. The assignment of the ^{13}C HFS constants was supported by the results of theoretical calculations, using the classical, semi-empirical Karplus-Fraenkel approach, as well as quantum chemical procedures based on density functional theory (DFT), representing the influence of the solvent by polarizable continuum models (PCM). The combined results suggest a consistent assignment of positions and signs for all five ^{13}C constants of GAS, providing a unique insight into the electron spin structure of this radical.

1. Introduction

Gallic acid (3,4,5-trihydroxybenzoic acid, GA) and many of its derivatives are widely present in numerous fruits and plants, where they represent a large family of secondary metabolites. Many of these metabolites, containing the gallate moiety, are essential phytochemicals known to participate in pharmacological activities, hereby being responsible for antioxidant, antiviral, and other important properties. For an introduction to the literature, see Ref. [1]. At an elevated pH, GA is oxidized by air to yield the unusually stable gallate semiquinone radical tri-anion [1,2] (GAS, Scheme 1). In this publication, we present the results of a detailed investigation of GAS by electron paramagnetic resonance (EPR) spectroscopy and by theoretical calculations.

The aim of the investigation is to determine and assign the ^{13}C HFS constants of GAS. The two aromatic protons at positions 2 and 6 give rise to a very intense 1:2:1 triplet in the EPR spectrum [1,2], but when amplifying the signal out of scale, numerous satellite lines appear, all deriving from the ^{13}C nuclei present in the radical in their natural abundance [2]. Actually, signals are observed from all seven carbon centers, enabling a unique insight into the electron spin structure of GAS.

However, assignment of the observed ^{13}C constants to individual positions in the radical is not straightforward. Theoretical investigations of the radical tri-anion in aqueous solution are difficult because of the strong influence of the polar and protic solvent medium. We shall apply two approaches: (1) We shall first attempt to adopt the classical theories of Das and Fraenkel [3] and Karplus and Fraenkel [4]. (2) We then apply modern quantum chemical procedures based on density functional theory.

(1) Das and Fraenkel [3] studied 1,4-benzosemiquinone and 2,5-dioxy-1,4-benzosemiquinone and had available proton as well as ^{13}C splittings at all positions in the radicals. They could thereby make a thorough test of the semiempirical Karplus-Fraenkel theory [4] relating the carbonyl ^{13}C splittings to the π-electron spin densities. We shall apply the classical Karplus-Fraenkel theory in order to see how far we can get in assigning the ^{13}C constants observed for GAS. If we permute the constants, using positive as well as negative sign to each constant, we are facing a calculation of 384 different possible assignments. The task becomes to single out only one, correct one.
(2) In a second attempt, the hyperfine coupling constants are studied by density functional theory (DFT) calculations, rep-

* Corresponding author.
E-mail address: spanget@ruc.dk (J. Spanget-Larsen).
§ Retired.

https://doi.org/10.1016/j.molstruc.2021.130663

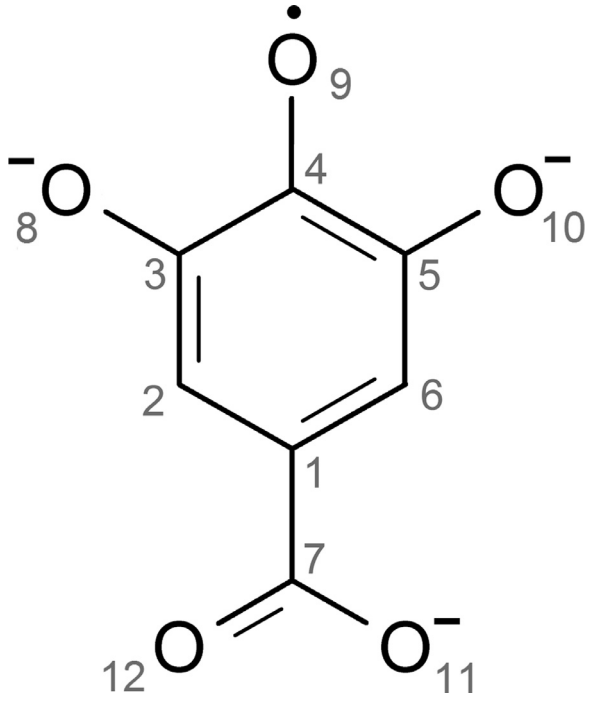

Scheme 1. Gallate semiquinone radical tri-anion (GAS) with the adopted atom numbering.

resenting the influence of the solvent by polarizable continuum models (PCM) [5]. Two PCM procedures were applied: the integral equation formalism PCM (IEFPCM) [6–9] and the isodensity PCM (IPCM) [10,11].

Detailed results are provided as Supplementary material, referred to in the ensuing text as S1–S4.

2. Experimental

Gallic acid (CAS 149-91-7) was commercially available (Fluka, AG) and used without further purification. The semiquinone radical was formed at room temperature in a water/ethanol alkaline solution by air oxidation at an elevated pH (solvent: 20 mm^3 80% ethanol v/v mixed with 5 mm^3 water adjusted with NaOH, pH = ca. 13). The EPR spectrum was run at the X-band on a Bruker ER 200 spectrometer with a modulation frequency of 12.5 kHz and equipped with a Gaussmeter for standardization. No accumulations were needed due to a very intense spectrum. The spectrum was stored digitally and "best fit" parameters were obtained by an iterative optimization procedure as described earlier [12]. By this procedure, the splitting constants, relative intensities, as well as different peak-to-peak linewidths for high and low field triplets for each individual spectrum were obtained (Table 1).

3. Theoretical calculations

Application of the semiempirical Karplus-Fraenkel theory [3,4] is described in Section 4.2 (details are provided as Supplementary material S1). Quantum chemical calculations were performed with the Gaussian16 software package [13] using density functional theory (DFT) with inclusion of a contribution from the solvent by means of polarizable continuum models (PCM) [5]. The B3LYP density functional [14,15] has in previous studies been found to be a suitable functional for the calculation of hyperfine coupling constants [16–23], and the results reported in the following were obtained with the unrestricted version of this functional. A number of basis sets have been developed for the computation of hyperfine constants; a survey was published recently by Jakobsen and Jensen [21]. We have performed B3LYP calculations on GAS with several of the recommended basis sets: D95(d,p) [24], EPR-II [17], EPR-III [17], pcH-2 [21], and pcH-3 [21]. But the signs and the relative values of the computed ^{13}C constants were found to be rather insensitive to the choice of basis. The results reported in the ensuing sections were obtained primarily with the EPR-III basis set. This is a triple-zeta basis including diffuse functions, double *d*- and a single set of *f*-polarization functions, and with an enhanced *s*-part to optimize the description of the nuclear region [17]. Solvent effects were considered by using the IEFPCM [6-9] and the IPCM [10,11] solvation models. The IEFPCM calculations were performed with the default parameters for the solvent water [13]. In the IPCM, the number of angular points in the spherical grids around each atom were taken as $\phi = 40$ and $\theta = 20$, and the surface isodensity parameter IsoD and the dielectric constant ε were selected as described in Section 4.4.2. Optimizations of molecular geometries were performed with IEFPCM (S2), since Gaussian16 does not allow geometry optimizations with IPCM. Several IEFPCM calculations were performed within a mixed discrete-continuum model [5] with inclusion of a number of explicit solvent species in the solute cavity. These calculations were performed with B3LYP/EPR-II and were of a tentative nature; the results are qualitative and are not reported in detail. Atomic net charges and spin populations were estimated by the natural population analysis (NPA) [25].

4. Results and discussion

4.1. Observed spectrum

Fig. 1 shows the experimental spectrum of GAS. Because the radical is observed at an elevated pH the carboxyl and hydroxyl protons are all dissociated leaving the semiquinone as a tri-anion. The upper spectrum consists of a main 1:2:1 triplet from two equivalent protons and numerous satellite lines, all deriving from ^{13}C carbon atoms in naturally abundance. Because of in-pairs equivalence between two sets of carbon atoms, the seven ^{13}C atoms give rise to only five 1:2:1 1:2:1 satellite spectra, furnishing five HFS constants. The spectra are here shown as the simulated ones, **a** to **e**.

Table 1
Experimental ^{1}H and ^{13}C hyperfine coupling constants from Fig. 1 and peak-to-peak linewidth data obtained from the simulations. The simulations were performed with a resolution of 2.5 mG, coupling constant uncertainty ±5 mG.

Curve	$\|a(^{13}C)\|$ (G)	Linewidth of low field 1:2:1 triplet (G)	Linewidth of high field 1:2:1 triplet (G)	Intensity (relative)	Theoretical intensity (relative)	Deviation
a	0.952	0.084	0.097	2.37	2.216	6.9%
b	2.259	0.108	0.076	0.98	1.108	11.6%
c	3.470	0.080	0.072	1.07	1.108	3.4%
d	5.999	0.075	0.089	2.16	2.216	2.5%
e	7.733	0.087	0.123	1.10	1.108	0.7%
$\mathbf{a_H}$ =	1.088					

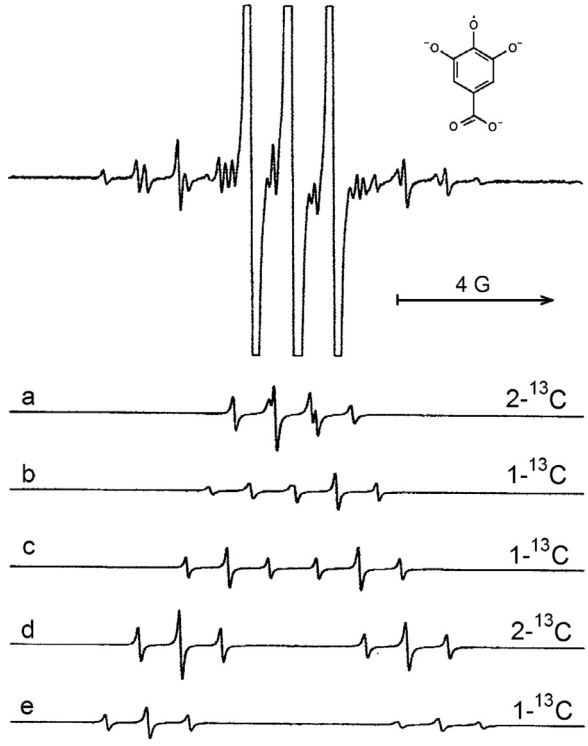

Fig. 1. Experimental spectrum from the gallate semiquinone tri-anion (GAS) with the main triplet [2H, 1:2:1] shown out of scale (top curve) and numerous satellite lines from seven ^{13}C atoms in their natural abundance. Due to pairwise equivalence, the seven ^{13}C atoms give rise to only five 1:2:1 1:2:1 satellite spectra (**a** to **e**), here shown as the simulated ones. Adapted with permission from Ref. [2], p. 25 (Copyright © 1985, CRC Press, Taylor & Francis Group).

Advanced simulations [12] as described above have furnished the data shown in Table 1. Due to the mentioned equivalence we have two sets of constants, the first one including the values 0.952 and 5.999 G with relative intensity 2 for the corresponding spectra. These values have to be assigned to the C2 (= C6) and C3 (= C5) positions. The second set, with relative intensity 1, consists of the constants 2.259, 3.470, and 7.733 G to be assigned to the positions C1, C4, and C7.

4.2. Karplus-Fraenkel theory

In order to get each individual constant assigned and obtain its sign, we shall use the theory by Karplus and Fraenkel [4]. This theory relates carbonyl ^{13}C splittings to π-electron spin densities via a number of $\sigma-\pi$ parameters. In case of a carbonyl group the parameters $Q_{CO}{}^{C}$ and $Q_{OC}{}^{C}$ give rise to the ^{13}C splittings from polarization through unpaired π-electrons on the carbon and oxygen atoms, respectively. For a CC' bond the corresponding parameters are termed $Q_{CC'}{}^{C}$ and $Q_{C'C}{}^{C}$ and the contribution from the 1s electron, S^{C}.

The theory involves in the present case eight π-spin densities (ρ_i) and yield five equations for the five HFS constants:

$$a_1{}^{C} = \left(S^{C} + 3Q_{CC'}{}^{C}\right)\rho_1 + Q_{CC'}{}^{C}(2\rho_2 + \rho_7) \quad (1)$$

$$a_2{}^{C} = \left(S^{C} + 2Q_{CC'}{}^{C}\right)\rho_2 + Q_{C'C}{}^{C}(\rho_1 + \rho_3) \quad (2)$$

$$a_3{}^{C} = \left(S^{C} + 2Q_{CC'}{}^{C} + Q_{CO}{}^{C}\right)\rho_3 + Q_{C'C}{}^{C}(\rho_2 + \rho_4) + Q_{OC}{}^{C}\rho_8 \quad (3)$$

$$a_4{}^{C} = \left(S^{C} + 2Q_{CC'}{}^{C} + Q_{CO}{}^{C}\right)\rho_4 + 2Q_{C'C}{}^{C}\rho_3 + Q_{OC}{}^{C}\rho_9 \quad (4)$$

$$a_7{}^{C} = \left(S^{C} + Q_{CC'}{}^{C} + 2Q_{CO}{}^{C}\right)\rho_7 + Q_{C'C}{}^{C}\rho_1 + 2Q_{OC}{}^{C}\rho_{11} \quad (5)$$

For the parameters we use the semiempirical ones obtained by Das and Fraenkel [3]:

$$S^{C} = -12.7\ \text{G},\quad Q_{CC'}{}^{C} = +14.4\ \text{G},\quad Q_{C'C}{}^{C} = -13.9\ \text{G},\quad Q_{CO}{}^{C} = +17.7\ \text{G},\quad Q_{OC}{}^{C} = -27.1\ \text{G}.$$

At this point it should be noticed that these parameters are obtained from two planar semiquinone radicals. Our radical is not necessarily planar because of the possible out-of-plane twist of the carboxylate group (see Section 4.4) for which the parameters might need to be adjusted. We shall discuss this later. In addition to the above equations we shall apply the McConnell equation [26] with $Q_{CH}{}^{C} = -26$ G,

$$a_2{}^{H} = Q_{CH}{}^{H}\rho_2 \quad (6)$$

Finally, we have for the conservation of π-spin density the equation,

$$\sum{}^{\rho_i} = 1. \quad (7)$$

where the summation runs over all eight different atoms in the π-electron system, including equivalent atoms.

4.2.1. Assignment by semiempirical spin density calculations

In order to perform spin density calculations we need 8 equations for the 5 different ^{13}C atoms and 3 different ^{17}O atoms. We have five ^{13}C HFS constants (cf. Eqs. (1)–(5)), one proton constant (6), and the conservation Eq. (7), hereby lacking one equation. We therefore proceed as follows. We assume we know the π-spin density at C1 (see below) and derive equations for all other spin densities as a function of this density (ρ_1). By insertion of relevant parameters in the above equations we obtain

$$\rho_2 = -0.0418 \quad (8)$$

$$\rho_3 = -\rho_1 - 0.0485 - 0.0719a_2{}^{C} \quad (9)$$

$$\rho_7 = 2.1942\rho_1 + 0.0837 - 0.0719a_1{}^{C} \quad (10)$$

$$\rho_{11} = 1.2455\rho_1 + 0.0572 - 0.0493a_1{}^{C} - 0.0185a_7{}^{C} \quad (11)$$

$$\rho_4 = 0.8274 - 1.8148\rho_1 + 0.1395a_1{}^{C} + 0.2043a_2{}^{C} + 0.0302\left(2a_3{}^{C} + a_4{}^{C} + a_7{}^{C}\right) \quad (12)$$

The spin density ρ_4 has been obtained by including the normalization condition (7). The last two ρ_8 and ρ_9 are now easily obtained from (3) and (4), respectively.

We can now calculate a set of spin densities from the equations just found, then permute the constants to a new assignment and continue to see whether some of the assignments for the five ^{13}C constants can be discarded as being meaningless. By this procedure many calculated densities become close to 1 or larger than 1 and the corresponding assignment can as a rule be discarded. However, since we are facing a task with 384 different assignments, it has turned out to be a more fruitful procedure to include calculation of the two oxygen HFS constants $a_8{}^{O}$, $a_9{}^{O}$, even though these constants are not known experimentally. The constants may be calculated by an equation proposed by Broze, Luz, and Silver [27] being similar to the equations by Karplus et al. The equations for O8 and O9 run:

$$a_8{}^{O} = Q_{OC}{}^{O}\rho_8 + Q_{CO}{}^{C}\rho_3 \quad (13)$$

$$a_9{}^{O} = Q_{OC}{}^{O}\rho_9 + Q_{CO}{}^{C}\rho_4$$

For the Q parameters we shall apply $Q_{CO}{}^{C} = +17.7$ G, the value used before, and $Q_{OC}{}^{O} = -40$ G, the value used by Broze et al. [27].

Since we have a semiquinone radical with an unpaired electron distributed over 12 atoms, we might assume there exists a numerical upper limit for the sizes of the two ^{17}O constants (cf. 7.733 G being the largest among the ^{13}C constants). We shall assume that an assignment can be discarded in case the calculated numerical value of either one of $a_8{}^{O}$ and $a_9{}^{O}$ exceeds 10 G or we get unusually large spin densities, i.e., our conditions for discarding an assignment are:

$$\left|a_8{}^{O}\right| > 10 \text{ G or } \left|a_9{}^{O}\right| > 10 \text{ G or } \rho_i > 0.9. \quad (14)$$

We now proceed as follows: For the unknown density ρ_1 preliminary calculations with ρ_1 lying in the range $-0.3 < \rho_1 < +0.3$ clearly indicates that this density has to be positive. Accordingly, we shall apply the center value on the positive side $\rho_1 = 0.15$ (this value turns out to be close to the NPA value $\rho_1 = 0.16$, see Section 4.4.2).

We begin the calculations by first considering the set of constants 5.999 and 0.952 G to be assigned to the carbon atoms C2 and C3, then the set of constants 7.733, 3.470 and 2.259 G to be assigned to the carbon atoms C1, C4 and C7. Each individual calculation is straight forward, but because the 384 different assignments require the same number of calculations the process is comprehensive. We shall leave the details to Supplementary material S1 and only illustrate the procedure by some examples.

We start by placing the constant +5.999 G at C2, the constant 0.952 G (±) then being at C3. No matter what assignments we choose for the remaining constants, being negative or positive, $a_8{}^{O}$ and $a_9{}^{O}$ show up with completely meaningless values in all calculations. In fact the 96 permutations which can be formed lead to

$$a_8{}^{O} > +27 \text{ G and } a_9{}^{O} < -41 \text{ G}$$

If we then assign +5.999 to C3, the constant 0.952 G (±) being placed at C2, the analysis becomes more intricate, but the results are the same, all 96 assignments can be discarded. We have hereby ruled out half of the possible assignments (= 192) with the result, that the constant 5.999 has to be negative.

We next repeat the calculations assigning –5.999 first to C2 and subsequently to C3 and permute all other constants. Only when assigned to C2 do we get meaningful results. We can thus rule out the 96 permutations with the constant –5.999 placed at C3 and state that

$$a_2{}^{C} = -5.999 \text{ G and } a_3{}^{C} = \pm 0.952 \text{ G}$$

Turning to the second set of constants, 7.733, 3.470, 2.259, there remain 96 permutations to consider. From the calculations it is obvious, that 7.733 G (±) placed at the carbon atoms C4 or C7 breaks the condition (14) in all 64 cases, no matter how we assign the other two constants, i.e., the constant 7.733 has to be assigned to C1. Assigning the value –7.733 to C1 leads to the following results for the 16 possible permutations,

$$a_8{}^{O} < -42 \text{ G and } a_9{}^{O} > +68 \text{ G},$$

emphasizing that the value 7.733 has to be positive, i.e.

$$a_1{}^{C} = +7.733 \text{ G}$$

Out of 384 permutations we end up with the task to assign the values 2.259 and 3.470 to C3 and C4 or vice versa. However, the calculations alone cannot yield an unequivocal answer, mainly because of the closeness in magnitude of the two values. The same concerns whether the two values, together with the smallest constant (0.952 G) at C3 are positive or negative. Accordingly, we shall turn to the observed asymmetric linewidth broadening, to see whether we can confirm the above conclusions.

4.3. Linewidth analysis

De Boer and Macker [28] were the first to show, that signs of ^{13}C splittings may be determined by utilizing the differences in linewidths observed between low and high field ^{13}C satellite lines. By making appropriate assumptions, the details of which shall not be stated here [29,30], it can be shown that

$$a_i{}^{C}/\left|a_i{}^{C}\right| = \pm\rho_i/|\rho_i| \quad (15)$$

where the upper sign holds if the high-field satellite is broader than the low-field satellite, and vice versa. ρ_i is the local π-electron spin density on atom i.

We look at the two largest constants, 5.999 and 7.733 G from the curves **d** and **e** (Fig. 1) and see whether we can confirm the results obtained so far. All six lines are easily seen for both curves, but notice that the two innermost lines of **e** are coincident with the two outermost lines of **c**. Still, the simulated fit for **d** and **e** is nearly perfect (cf. Table 1). The curves exhibit broader lines to high field meaning the upper sign in (15) holds. From above we have $\rho_1 = +0.15$ and $\rho_2 = -0.042$, meaning $a_1{}^{C}$ should be positive and $a_2{}^{C}$ negative, in complete agreement with the calculations and analyses made previously. The result is also in line with the theory [31] stating that the widths of the lines vary approximately as the first power of the local spin density. Looking at Table 1 we see that curve **e** has a 36 mG broadening difference, approximately three times that of curve **d** (3 × 14 mG) in fair agreement with the similar relative differences in π-spin densities.

For the curves **a, b** and **c** (Fig. 1) we are facing a much more subtle analysis. All three curves compete about the same narrow space around the main proton lines, and nearly half of their 18 lines (3 × 6) are overlapped by these three strong lines. In case of **b** only the two outermost lines are seen, in line with the simulation for this curve giving a 12% relative intensity deviation (Table 1). Furthermore, the **b** curve differs from curves **a** and **c** by having the largest asymmetric broadening (32 mG), compared to 13 and 8 mG for **a** and **c**, respectively.

However, Eq. (15) is valid for a planar system, but the carboxylate group in GAS is likely to be twisted more or less out-of-plane of the benzene ring (see Section 4.4). Furthermore, the Karplus-Fraenkel parameters used above are obtained empirically for aromatic CC and CO carbonyl bonds. Use of these parameters in the above calculations seems reasonably justified, since we have focused on the carbonyl constants from the O8, O9, and O10 oxygens. Use of the same parameters in case of our carboxylate group might lead to erroneous results. Five parameters are needed in order fully to cope with a carboxylate group. Since we have no way of checking the validity of the results we might obtain, we shall not go any further into adjusting these five $\sigma-\pi$ parameters.

The results of the semiempirical analyses can thus be summarized:

$$a_1{}^{C} = +7.733 \text{ G and } a_2{}^{C} = -5.999 \text{ G}$$

$$a_3{}^{C} = +0.952 \text{ G or } a_3{}^{C} = -0.952 \text{ G}$$

$$a_4{}^{C}/a_7{}^{C} = 2.259/3.470\text{G or } 3.470/2.259\text{G},$$

the signs of the values being unknown.

4.4. Quantum chemical calculations

4.4.1. IEFPCM

In this model, the solute cavity is defined as a superposition of interlocked atomic spheres with fixed radii, using a continu-

Table 2
^{13}C, ^{1}H, and ^{17}O hyperfine coupling constants (G) predicted with B3LYP/EPR-III and the solvation models IEFPCM and IPCM. Experimental values (Sections 4.2 and 4.3) are included for comparison.

	IEFPCM[a] Planar	IEFPCM[a] Non-planar[c]	IPCM[b] Planar	IPCM[b] Non-planar[c]	Expt.
a_1^C	+5.836	+5.713	+6.167	+6.030	+7.733
$a_2^C = a_6^C$	−5.009	−4.764	−5.281	−5.007	−5.999
$a_3^C = a_5^C$	−0.803	−1.095	−0.380	−0.729	±0.952
a_4^C	−0.334	+0.521	+0.697	+1.206	±2.259 or ±3.470
a_7^C	−2.541	−2.194	−2.424	−2.361	±3.470 or ±2.259
$a_2^H = a_6^H$	+1.414	+1.117	+1.495	+1.226	+1.088
$a_8^O = a_{10}^O$	−4.263	−3.819	−3.923	−3.670	
a_9^O	−7.516	−8.171	−7.254	−7.837	
$a_{11}^O = a_{12}^O$	−0.315	−0.815	−0.309	−0.927	

[a] Solvent = water (S2).
[b] IsoD = 0.0025, ε = 30 (S3,S4).
[c] Carboxylate group twisted out-of-plane by 90°.

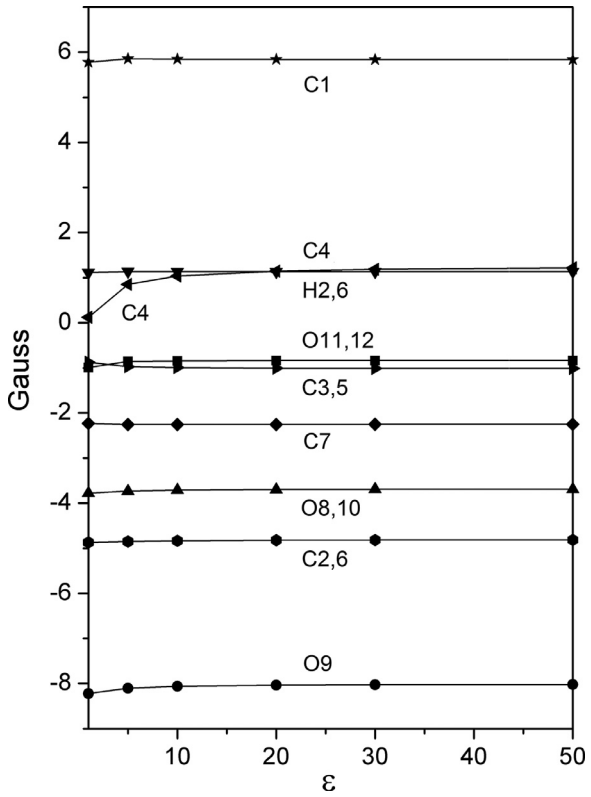

Fig. 2. HFS constants for positions in the gallate semiquinone radical tri-anion (GAS) computed for the non-planar C_{2v} symmetrical conformation with B3LYP/EPR-III and the IPCM solvation model as a function of the solvent parameter ε (constant IsoD = 0.0025).

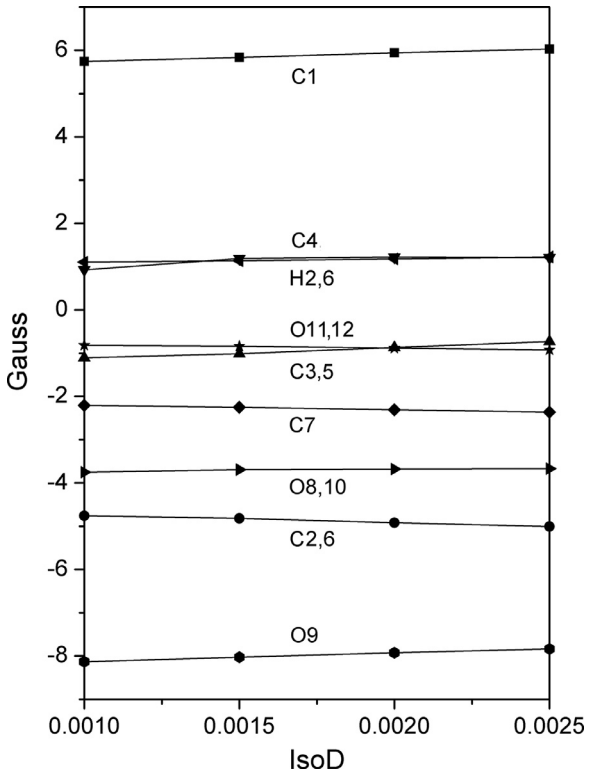

Fig. 3. HFS constants for positions in the gallate semiquinone radical tri-anion (GAS) computed for the non-planar C_{2v} symmetrical conformation with B3LYP/EPR-III and the IPCM solvation model as a function of the cavity boundary parameter IsoD (constant ε = 30).

ous surface charge formalism [6–9]. This procedure allows optimization of the molecular structure in the solvent reaction field. Full B3LYP/EPR-III geometry optimization of GAS in water predicts a slightly non-planar equilibrium structure with the carboxylate group twisted 4° out of the plane of the benzene ring (S2). The coupling constants predicted for the equilibrium structure are essentially identical to those predicted for the structure optimized under the assumption of a perfectly planar C_{2v} symmetrical geometry (S2). The constants computed for the latter structure are listed in Table 2.

It is expected that specific solvation of the tri-anion in protic solvents like water and alcohols will lead to a significant twisting of the carboxylate group in order to accommodate intermolecular hydrogen bonds with the solvent molecules. Table 2 also lists the constants predicted for the structure optimized under the assumption of a non-planar C_{2v} symmetrical geometry, i.e., with the dihedral angle of the carboxylate group equal to 90° (S2). Most of the predicted constants are not strongly affected by the twisting, but the proton constant is reduced from 1.41 G in the planar to 1.12 G in the non-planar structure. The latter value is in much better agreement with the observed proton constant, 1.09 G. This suggests that the non-planar structure may be a better model for GAS in aqueous solution. Also, the ^{13}C constant a_4^C is affected; it is predicted to be small and changes sign when passing from the planar to the non-planar structure.

The analyses described in Sections 4.2 and 4.3 led to unambiguous assignment of the ^{13}C constants a_1^C and a_2^C (= a_6^C). The theoretical values calculated with IEFPCM agree with the assigned

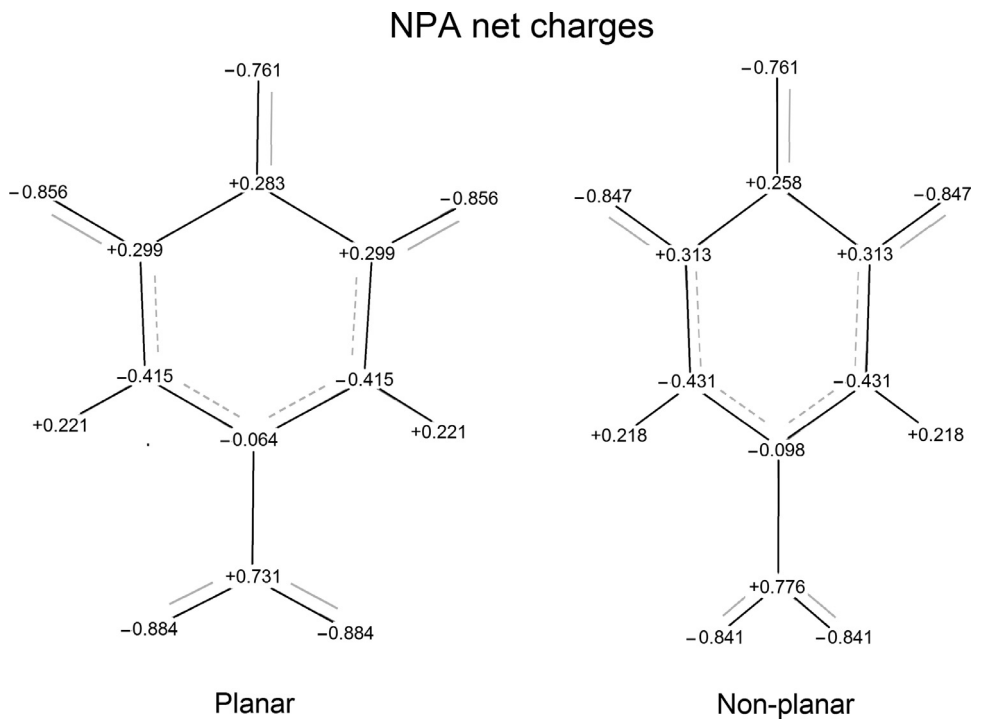

Fig. 4. Natural atomic net charges computed for planar and non-planar gallate semiquinone radical tri-anion (GAS). The charges correspond to the data listed in Table 2, columns "IPCM Planar" and "IPCM Non-planar".

signs and relative magnitudes for these constants, irrespective of the assumed twisting angle (Table 2). The abovementioned analyses also showed that the constant a_3^C (= a_5^C) has the smallest magnitude of the five observed ^{13}C constants, but the assignment of its sign was left open. The constant calculated with IEFPCM is not in perfect agreement with the observed relative magnitude, but indicates the assignment of a negative sign. The analyses outlined in Sections 4.2 and 4.3 were not able to distinguish between the magnitudes and the signs of the remaining two ^{13}C constants, a_4^C and a_7^C. The magnitude of a_7^C is predicted to be larger than that of a_4^C (Table 2). As mentioned above, the calculated sign of a_4^C depend on the assumed twisting angle, but the sign of a_7^C is predicted to be negative, irrespective of the twisting.

However, the pure IEFPCM is likely to be inadequate for GAS in aqueous solution. The PCM approach is based on the assumption that the electronic structure of the solute molecule is insignificantly affected by interactions with individual solvent species. But semiquinone radical anions tend to be strongly influenced by specific solute-solvent interactions in protic media [32–37]. An adequate model of GAS in aqueous solution must consider interactions with individual solvent molecules. A proper theoretical treatment should probably use advanced molecular dynamics procedures [38–40], but such procedures are presently not within our reach. To obtain a qualitative estimate of the possible impact of specific interactions, we have experimented with a variety of mixed discrete-continuum models [5], including up to ten water molecules and three sodium counter ions in the solute cavity. The geometry of each model system was optimized with IEFPCM without any restrictions. In general, the predicted constants were not drastically affected by the inclusion of the solvent clusters. The predicted magnitude and sign of a_4^C varied with the details of the resulting solute-solvent clusters, but the value obtained for a_7^C was consistently large and negative. Hence, the results of the tentative discrete-continuum calculations tend to support the assignment of a negative value for a_7^C, as predicted also for the "un-clustered" radical (Table 2).

4.4.2. IPCM

As described above, the solute cavity in the IEFPCM is constructed as a superposition of atomic spheres with fixed radii. The default values for these radii, optimized for neutral molecules, are not necessarily adequate for a triply charged anion like GAS. In the IPCM, the boundary of the cavity is defined as an isodensity surface, i.e., a surface of constant electronic density. This surface is relaxed in the solvent reaction field and thus reflects the reactive shape of the solute molecule. In this respect, IPCM may be more suitable than IEFPCM for a radical like GAS.

The IPCM calculation requires input of two parameters, the surface isodensity value (IsoD) and the dielectric constant (ε) of the medium. Increasing the values of any of the two parameters leads to an increase of the strength of the solvent reaction field. In previous applications on semiquinones, it has been possible to simulate the total impact of a protic solvent on the coupling constants by appropriate adjustment of the two model parameters [18,22]. This amounts to the assumption that the rapidly changing formation and breaking of complexes between solute and solvent molecules can be considered as giving rise to an effective electrostatic solvent field at the position of the solute, and thus can be simulated in an average manner within the continuum picture [18,22,36].

We have performed a survey of the influence of the parameters IsoD and ε on the predicted hyperfine coupling constants of GAS. The results obtained with the non-planar C_{2v} symmetrical GAS geometry computed with IEFPCM are shown in Figs. 2 and 3. Fig. 2 shows the computed constants as a function of ε in the range 1–50, keeping IsoD equal to 0.0025 (electrons Bohr^{-3}), and Fig. 3 displays the constants as a function of IsoD in the range 0.0010–0.0025 for constant ε equal to 30. It is apparent that the computed constants are quite insensitive to the impact of the solvent field, except for a shift of a_4^C for the initial values of ε in Fig. 2. No crossing of the curves for the ^{13}C constants are observed, no reordering of the relative values. This is in striking contrast to the results of similar IPCM calculations for other semiquinones where the predicted impact of the solvent is profound, completely

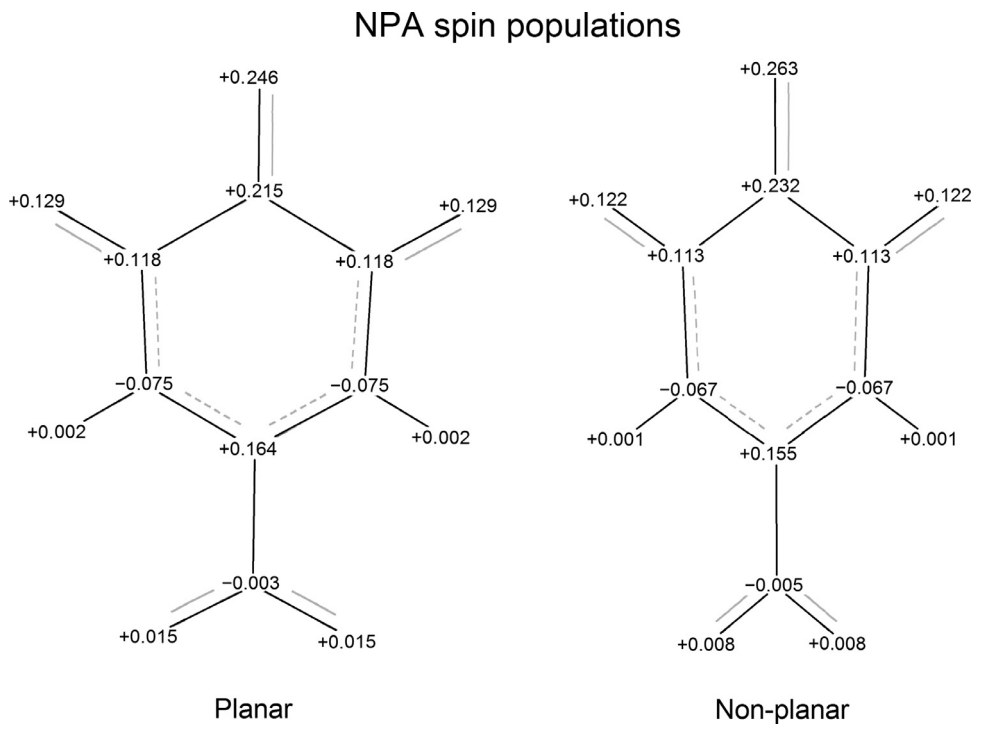

Fig. 5. Natural atomic spin populations computed for planar and non-planar gallate semiquinone radical tri-anion (GAS). The populations correspond to the data listed in Table 2, columns "IPCM Planar" and "IPCM Non-planar".

rearranging the relative magnitudes and signs of the ^{13}C constants [18,22]. The insensitivity of the coupling constants of GAS can probably be explained by the circumstance that the excess negative charge in this tri-anion is localized on the five exposed oxygen centers, rather uniformly distributed on the periphery of the solute species (Fig. 4). The solvation seems to affect the electronic structure in a fairly uniform manner; the gradient of the solvent reaction field is evidently too small to rearrange the relative values of the coupling constants.

The IPCM results obtained with IsoD = 0.0025 and ε = 30 for the planar and the non-planar geometries are included in Table 2 (detailed results are provided as S3 and S4). In general, the results are not drastically affected by the twist angle, similar to the case of IEFPCM. This observation may be explained in part by the calculated NPA atomic spin populations shown in Fig. 5. It is apparent that the predicted spin populations on the carboxylate group are very small in both conformations. Apart from the spin density on the protons, the overall spin distribution is affected only to a minor degree by rotation of the COO^- group.

The IPCM results (Table 2) are in agreement with the previously established assignments of $a_1{}^C$ and $a_2{}^C$ (= $a_6{}^C$), and suggest the assignment of a negative sign for the smallest constant $a_3{}^C$ (= $a_5{}^C$), and positive and negative signs for $a_4{}^C$ and $a_7{}^C$, respectively, with $|a_4{}^C| < |a_7{}^C|$. As shown in Fig. 6, adopting these assignments leads to a satisfactory linear correlation between experimental and calculated values: The observed constants are reproduced to an RMS standard deviation of 0.43 G by the scaling relation

$$a^C(\text{obsd}) = 1.283 \cdot a^C(\text{theor}).$$

On the other hand, it is apparent that the computed constants significantly underestimate the observed magnitudes. We have presently no obvious explanation for this. But it should be kept in mind that the theoretical description of a highly charged species like the gallate radical tri-anion in an aqueous medium is a difficult task.

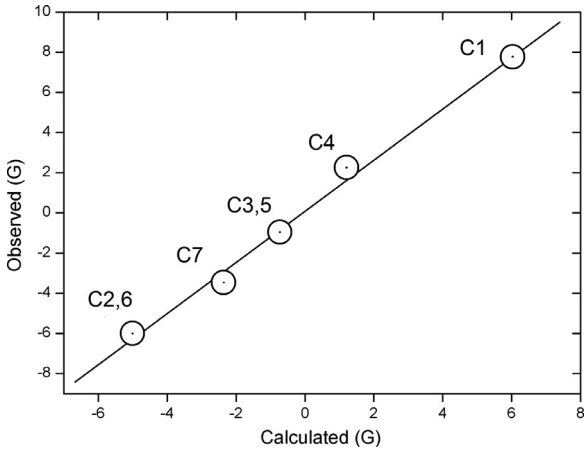

Fig. 6. Correlation of observed and calculated ^{13}C HFS constants for positions in the gallate semiquinone radical tri-anion (GAS) according to the suggested assignment (see main text). The calculated constants are listed in the column "IPCM Non-planar" in Table 2. The straight line indicates the least squares scaling relation Y = 1.283 X (R = 0.995, SD = 0.43 G).

5. Concluding remarks

The determination of the spin-density distribution in aromatic free radicals has in many studies been based on proton HFS constants determined by EPR. In the case of aromatic hydrocarbons, this is often an acceptable situation. But when it comes to the investigation of semiquinone free radicals, derived either from benzoquinols or benzoquinones [2], the situation is quite different, due to the many "blind" spots from the presence of OH groups and other substituents such as COOH groups. Furthermore, to gain stability, semiquinone radicals are often generated at an elevated pH in order to dissociate the COOH and OH protons, leaving only the CH protons to be observed, often few in numbers.

The present EPR study of the gallate semiquinone radical trianion (GAS) has furnished a complete mapping of the five HFS constants derived from all seven carbon positions via naturally occurring ^{13}C isotopes. Three constants have been unequivocally assigned by way of the classical, semi-empirical Karplus-Fraenkel theory with determination of the signs for the two largest constants. These signs were further confirmed by detailed linewidth analyses. The assignment of the two remaining constants by this approach were inconclusive, as well as the sign determination of the three smallest constants.

In a different theoretical approach, the HFS constants of GAS were calculated by density functional theory (DFT). These calculations, with inclusion of a contribution from the solvent by means of polarizable continuum models (PCM), led to fair agreement with the results of the Karplus-Fraenkel analysis and with the experimental evidence. As shown in Fig. 6, adopting the assignment corresponding to the relative magnitudes and the signs predicted with B3LYP/EPR-III + IPCM leads to a satisfactory correlation between calculated and observed ^{13}C constants. However, the predicted magnitudes consistently underestimate the observed values. This may be related to the difficulties associated with an adequate description of the influence of the solvent on the semiquinone trianion in aqueous solution.

A drawback in this study is the lack of ^{17}O data. All ^{1}H and ^{13}C positions are covered, but the absence of three ^{17}O HFS constants from five oxygen atoms makes us unable to test and possibly refine the Karplus-Fraenkel parameters and test the predicted ^{17}O hfs constants presented in Table 2. Due to costly and time consuming synthesis, rather few HFS data from enriched quinones or quinols have been reported [2]. Exchange reactions may be part of the answer, as seen with cases of deuterium exchange [1] or use of enriched alcohols in exchanging methoxy or ethoxy groups [12].

Declaration of Competing Interest

The authors declare that they have no known competing financial interests or personal relationships that could have appeared to influence the work reported in this paper.

CRediT authorship contribution statement

Jens Arne Pedersen: Conceptualization, Methodology, Investigation, Resources, Formal analysis, Writing - original draft, Writing - review & editing. **Jens Spanget-Larsen:** Conceptualization, Methodology, Investigation, Formal analysis, Visualization, Writing - original draft, Writing - review & editing.

Acknowledgments

The authors are grateful to J. R. Bolton for helpful advice.

Supplementary materials

Supplementary material associated with this article can be found, in the online version, at doi:10.1016/j.molstruc.2021.130663.

References

[1] A.C. Eslami, W. Pasanphan, B.A. Wagner, G.R. Buettner, Free radicals produced by the oxidation of gallic acid: an electron paramagnetic resonance study, Chem. Centr. J. 4 (2010) 15.
[2] J.A. Pedersen, Handbook of EPR Spectra from Quinones and Quinols, CRC Press, Boca Raton, FL, 1985 (eBook 2018).
[3] M.R. Das, K. Fraenkel, Electron spin resonance of semiquinones: spin-density distribution and carbonyl sigma-Pi parameters, J. Chem. Phys. 42 (1965) 1350–1360.
[4] M. Karplus, G.K. Fraenkel, Theoretical interpretation of Carbon-13 hyperfine interactions in electron spin resonance spectra, J. Chem. Phys. 35 (1961) 1312–1323.
[5] J.B. Foresman, Æ. Frisch, Exploring Chemistry With Electronic Structure Methods, Third Edition, Gaussian, Inc., Wallingford CT, 2015 Chapter 5, Modelling Chemistry in Solution.
[6] S. Miertuš, E. Scrocco, J. Tomasi, Electrostatic interaction of a solute with a continuum. A direct utilizaion of AB initio molecular potentials for the prevision of solvent effects, Chem. Phys. 55 (1981) 117–129.
[7] J. Tomasi, M. Persico, Molecular interactions in solution: an overview of methods based on continuous distributions of the solvent, Chem. Rev. 94 (1994) 2027–2094.
[8] C.J. Cramer, D.G. Truhlar, Implicit solvation models: equilibria, structure, spectra, and dynamics, Chem. Rev. 99 (1999) 2161–2200.
[9] G. Scalmani, M.J. Frisch, Continuous surface charge polarizable continuum models of solvation. I. General formalism, J. Chem. Phys. 132 (2010) 114110.
[10] K.B. Wiberg, P.R. Rablen, D.J. Rush, T.A. Keith, Amides. 3. Experimental and theoretical studies of the effect of the medium on the rotational barriers for *N,N*-Dimethylformamide and *N,N*-Dimethylacetamide, J. Am. Chem. Soc. 117 (1995) 4261–4270.
[11] J.B. Foresman, T.A. Keith, K.B. Wiberg, J. Snoonian, M.J. Frisch, Solvent Effects 5. The influence of cavity shape, truncation of electrostatics, and electron correlation on ab initio reaction field calculations, J. Phys. Chem. 100 (1996) 16098–16104.
[12] V. Axelsen, J.A. Pedersen, Electron spin resonance as an analytical tool, J. Chem. Soc., Faraday Trans. I 83 (1987) 107–112.
[13] M.J. Frisch, G.W. Trucks, H.B. Schlegel, G.E. Scuseria, M.A. Robb, J.R. Cheeseman, G. Scalmani, V. Barone, G.A. Petersson, H. Nakatsuji, X. Li, M. Caricato, A.V. Marenich, J. Bloino, B.G. Janesko, R. Gomperts, B. Mennucci, H.P. Hratchian, J.V. Ortiz, A.F. Izmaylov, J.L. Sonnenberg, D. Williams-Young, F. Ding, F. Lipparini, F. Egidi, J. Goings, B. Peng, A. Petrone, T. Henderson, D. Ranasinghe, V.G. Zakrzewski, J. Gao, N. Rega, G. Zheng, W. Liang, M. Hada, M. Ehara, K. Toyota, R. Fukuda, J. Hasegawa, M. Ishida, T. Nakajima, Y. Honda, O. Kitao, H. Nakai, T. Vreven, K. Throssell, J.A. Montgomery Jr., J.E. Peralta, F. Ogliaro, M.J. Bearpark, J.J. Heyd, E.N. Brothers, K.N. Kudin, V.N. Staroverov, T.A. Keith, R. Kobayashi, J. Normand, K. Raghavachari, A.P. Rendell, J.C. Burant, S.S. Iyengar, J. Tomasi, M. Cossi, J.M. Millam, M. Klene, C. Adamo, R. Cammi, J.W. Ochterski, R.L. Martin, K. Morokuma, O. Farkas, J.B. Foresman, D.J. Fox, Gaussian16, Revision A.03, Gaussian, Inc., Wallingford CT, 2016.
[14] A.D. Becke, Density-functional thermochemistry. III. The role of exact exchange, J. Chem. Phys. 98 (1993) 5648–5652.
[15] C. Lee, W. Yang, R.G. Parr, Development of the Colle-Salvetti correlation-energy formula into a functional of the electron density, Phys. Rev. B 37 (1988) 785–789.
[16] C. Adamo, V. Barone, A. Fortunelli, Validation of self-consistent hybrid density functionals for the study of structural and electronic characteristics of organic radicals, J. Chem. Phys. 102 (1995) 384–393.
[17] V. Barone, Structure, magnetic properties and reactivities of open-shell species from density functional and self-consistent hybrid methods, in: Recent Advances in Density Functional Methods, Vol. 1, Part I, D. P. Chong (Ed.), World Scientific Publ. Co., Singapore, 1995, pp. 287-334.
[18] M. Langgård, J. Spanget-Larsen, The strong influence of the solvent on the electron spin resonance spectra of semiquinone radical anions. I. A theoretical investigation of the hyperfine constants of 1,2- and 1,4-benzosemiquinone by using density functional theory and polarizable continuum solvation models, J. Mol. Struct. (Theochem) 431 (1998) 173–180.
[19] V. Barone, P. Cimino, E. Stendardo, Development and Vvlidation of the B3LYP/N07D computational model for structural parameter and magnetic tensors of large free radicals, J. Chem. Theory Comput. 4 (2008) 751–764.
[20] L. Hermosilla, J.M. García de la Vega, C. Sieiro, P. Calle, DFT calculations of isotropic hyperfine coupling constants of nitrogen aromatic radicals: the challenge of nitroxide radicals, J. Chem. Theory Comput. 7 (2011) 169–179.
[21] P. Jakobsen, F. Jensen, Probing basis set requirements for calculating hyperfine coupling constants, J. Chem. Phys. 151 (2019) 174107.
[22] J. Spanget-Larsen, Chrysazin semiquinone radical anion. A theoretical study of the influence of the solvent on the electron spin resonance spectrum, Comput. Theor. Chem. 1185 (2020) 112878.
[23] J. Spanget-Larsen, Semiquinone radical anions derived from 2,3-dimethylchrysazin,7-deoxyaklavinone, and aclacinomycin T. Computational studies of the influence of aprotic and protic solvents on the electron spin resonance spectra, J. Mol. Liquids 320 (2020) 114508.
[24] T.H. Dunning, Jr., P.J. Hay, in: Modern Theoretical Chemistry, Vol. 3, H. F. Schaefer III (Ed.), Plenum, New York, 1976, pp. 1-28.
[25] A.E. Reed, R.B. Weinstock, F. Weinhold, Natural-population analysis, J. Chem. Phys. 83 (1985) 735–746.
[26] H.M. McConnell, Indirect hyperfine interactions in the paramagnetic resonance spectra of aromatic free radicals, J. Chem. Phys 24 (1956) 764–766.
[27] M. Broze, Z. Luz, B.L. Silver, Oxygen-17 hyperfine splitting constants in ESR spectra of p-semiquinone-^{17}O, J. Chem. Phys. 46 (1967) 4891–4902.
[28] E. de Boer, E.L. Mackor, Sign of C^{13} coupling constants in aromatic free radicals, J. Chem. Phys. 38 (1963) 1450–1452.
[29] J.H. Freed, G.K. Fraenkel, Theory of linewidths in electron spin resonance spectra, J. Chem. Phys. 39 (1963) 326–348.
[30] J.H. Freed, G.K. Fraenkel, Linewidth studies in electron spin resonance spectra: the *Para* and *Ortho* dinitrobenzene anions, J. Chem. Phys. 40 (1964) 1815–1829.
[31] J.R. Bolton, G.K. Fraenkel, Assignment of hyperfine splittings in electron spin resonance spectra by linewidth analyses, J. Chem. Phys. 41 (1964) 944–948.
[32] E.W. Stone, A.H. Maki, Electron spin resonance of semiquinones in aprotic solvents, J. Chem. Phys. 36 (1962) 1944–1945.

[33] J.A. Pedersen, Assignment of the h.f.s. constants of 1,4-benzosemiquinones by additivity rules. The free rotation of *t*-butyl groups, Mol. Phys. 28 (1974) 1031–1035.
[34] J. Spanget-Larsen, J.A. Pedersen, Solvent sensitivities of the hyperfine constants of methyl and *t*-Butyl-cubstituted 1,4-benzosemiquinones, J. Magn. Reson. 18 (1975) 383–389.
[35] J.A. Pedersen, J. Spanget-Larsen, The strong influence of the solvent on the spin distribution in 1,2-benzosemiquinones, Chem. Phys. Letters 35 (1975) 41–44.
[36] J. Spanget-Larsen, INDO calculations with inclusion of an effective solvent field. Application to benzosemiquinones, Theoret. Chim. Acta 47 (1978) 315–328.
[37] J. Spanget-Larsen, Assignment of the hyperfine constants of the 1,2-benzosemiquinone radical anion, Int. J. Quantum Chem. 18 (1980) 365–367.
[38] M.P. Allen, D.J. Tildesley, Computer Simulation of Liquids, Second edition, Oxford University Press, 2017.
[39] K. Bux, S.T. Moin, Solvation of cholesterol in different solvents: a molecular dynamics simulation study, Phys. Chem. Chem. Phys. 22 (2020) 1154–1167.
[40] A. Jindal, S. Vasudevan, Geometry of OH•••O interactions in the liquid state of linear alcohols from *ab initio* molecular dynamics simulations, Phys. Chem. Chem. Phys. 22 (2020) 6690–6697.